J Mater Sci: Mater Electron (2007) 18:1171–1177
DOI 10.1007/s10854-007-9276-7

Conductance analysis of (Co, Nb, Fe)-doped SnO_2 thick film gas sensors

Miguel Adolfo Ponce · Rodrigo Parra · Miriam S. Castro · Celso M. Aldao

Received: 4 October 2006 / Accepted: 3 April 2007 / Published online: 30 June 2007

Abstract Thick films prepared with undoped nanometric SnO_2 particles and with (Co, Nb, Fe)-doped SnO_2 were studied with the purpose of developing oxygen and carbon monoxide gas sensors. The ceramic powders were obtained through the Pechini method. The morphological characteristics were studied with SEM and TEM, after which, they were subjected to sensitivity tests under different atmospheres. A correlation was established between the microstructure of the material, the effects of the additives, and the electrical behavior. The response of the sensor could be explained as the result of the characteristics of the intergranular potential barriers developed at intergrains. It was determined that the SnO_2-doped films have a greater sensitivity between 200 °C and 350 °C.

1 Introduction

Tin dioxide (SnO_2) is an *n* type wide band gap semiconductor with a rutile type crystalline structure and with a low densification rate due to its high surface diffusion at low temperature and high SnO_2 partial pressure at high temperature. The latter constitutes the basis of its use in the field of gas sensors. The addition of Co_3O_4 to SnO_2 leads, after a thermal treatment at temperatures around 1300 °C, to a highly dense material with possible application as surge arrester [1]. Sensitizing effects by noble metals like Pd and Pt were discovered a long time ago [2, 3] and contributed to put the sensors into practice. The close relationship between gas sensing and catalytic properties verified in these systems caused a great interest in the sensitizing effects of those transition metal oxides, like Co_3O_4 and CuO, which are frequently used as catalysts in the oxidation of reducing gases [4].

The attractive feature of doped-SnO_2 based sensors is their sensitivity due to the presence of dopants. Concerning thick films, the gas sensitivity depent not only of the type of dopat but also on such basic material properties as microstructure and bulk electron concentration. For example, it is known that additions of Fe_2O_3 to the SnO_2 system lead to the similar mean grain size than the addition of CoO [5]. The effects of niobium oxide on SnO_2-based sensors have not been explored in detail and few articles on the subject are available in the literature. However, it is known that Nb_2O_5 increases the conductivity of SnO_2 since it behaves as an electron donor [6]. Some authors believe that niobium oxide also plays a fundamental role in powder morphology [7]. Fliegel et al. proposed that the addition of Nb_2O_5 to SnO_2 inhibits the particle growth producing powders with a large surface area [8, 9]. Behr et al. reported an effective way to improve the gas sensing properties of SnO_2 by multiple doping with Nb and Mn [10].

In this work, we present the advances achieved in (Co, Nb, Fe)-doped SnO_2 systems. The powders were prepared through the polymeric precursor method and calcined at temperatures around 650 °C to avoid grain growth. Such powders were used to make thick porous films with possible applications as gas sensors. The introduction of Nb_2O_5 to the $SnO_2 \cdot Co_3O_4$ system aimed to decrease the grain resistance and to improve the sensitivity of the films. The addition of Fe_2O_3 to the ternary system

M. A. Ponce (✉) · R. Parra · M. S. Castro · C. M. Aldao
Institute of Materials Science and Technology (INTEMA), University of Mar del Plata (UNMdP) and National Research Council (CONICET), J.B. Justo 4302, Mar del Plata, Buenos Aires B7608FDQ, Argentina
e-mail: mponce@fi.mdp.edu.ar

$SnO_2 \cdot Co_3O_4 \cdot Nb_2O_5$ was considered to examine the influence of this oxide in the electrical response of the films.

2 Experimental

Analytical grades of $SnCl_2 \cdot 2H_2O$ (Baker), $Co(CO\text{-}OCH_3)_2 \cdot 4H_2O$ (Acros Organics), and $Fe(NO_3)_3 \cdot 9H_2O$ (Sigma) were employed as sources of the cations of interest, whereas niobium was added as a Nb_2O_5 (Fluka AG) dispersion in ethanol. Tin dioxide was precipitated at pH 6.25 through the dropwise addition of ammonium hydroxide (NH_4OH) to an acid (HNO_3) solution of tin (II) chloride. A series of washings with deionised water were carried out until negative reaction of the filtrate with a concentrated silver nitrate ($AgNO_3$) solution. The obtained slurry, along with the required amounts of the dissolved additives, was added to a solution of citric acid in ethylene glycol in a 1:4 molar ratio. The mixtures were left at room temperature with constant stirring in a 24 h aging with the purpose of promoting the formation of the metallic citrates. Later, a concentrated solution of NH_4OH was slowly added until a crystalline solution was attained which was afterwards evaporated and heated to promote the polymerization. The solid was heated to 350 °C for 12 h in a beaker to burn off as much of the organics as possible. The resulting black brittle mass was ground, transferred into an alumina crucible of large surface and calcinated in an oven at 650 °C for 4 h. The remaining powders, which consisted in the mixture of oxides with the desired composition, were attrition milled with ZrO_2 balls to disintegrate large particles and agglomerates. The morphological characterization of the powder was performed by scanning electron microscopy (SEM), in a Topcon SM-300 microscope and with transmission electron microscopy (TEM) in a Philips CM200 instrument. The specific surface area was measured by N_2 adsorption/desorption BET isotherms by means of a Micromeritics ASAP 2010.

Following this procedure, the doped and non-doped films were arranged using screen printing for the electrical assays. A paste was prepared mixing the powders with an organic binder (glycerol) in a 2:1 ratio. Thick porous films were made by painting onto insulating alumina substrates on which electrodes with an interdigit shape had been previously deposited by sputtering. Finally, samples were thermally treated for 2 h in vacuum at 500 °C. The films were not calcined in air but in vacuum, in order to avoid the annihilation of oxygen vacancies [11].

The electrical measurements were carried out in a homemade testing gas chamber. The tests were carried out in order to determine the temperature of the highest sensitivity and the response time when the doped and non-doped films are exposed to oxygen. To analyze the possible conduction mechanisms involved, an impedance analyzer HP4284A, in the 20 Hz–1 MHz frequency range, was used. In temperature cycling experiments, the resistance was measured while rising and then decreasing the temperature from room temperature up to 475 °C at a rate of 2 °C/min with the sample kept in oxygen or carbon monoxide atmospheres. Resistance versus time curves were measured after a sudden change of the atmosphere from vacuum (10^{-4} mmHg) to oxygen (8.4 mmHg).

3 Results and discussion

Figure 1 shows a representative SEM micrograph of the synthesized powder, which presents a fine and homogeneous morphology. The small particle size lead to the formation of agglomerates of loosely bonded particles. With TEM (Fig. 2) it was confirmed that the powder consists in spheres of SnO_2 with a mean particle size below 50 nm and a specific surface area (BET) of 25 m^2/g.

By solving the Poisson's equation under the *depletion approximation*, or resorting to the Gauss theorem, the maximum grain boundary barrier height for a spherical grain is given by

$$\phi = \frac{q^2 N_d R^2}{6\varepsilon}, \tag{1}$$

where R is radius of the grain and N_d is the donor density. Based on reported data, Schottky barrier heights (φ) for these systems are around 1 eV and the donor density is in the order of 10^{24} m^{-3} [12, 13]. With these values, the critical grain size for which the grains are completely depleted is ~110 nm. It is expected then, that the depletion regions of the grains are overlapped and then the grains are completely depleted. Consistently with these calculations it

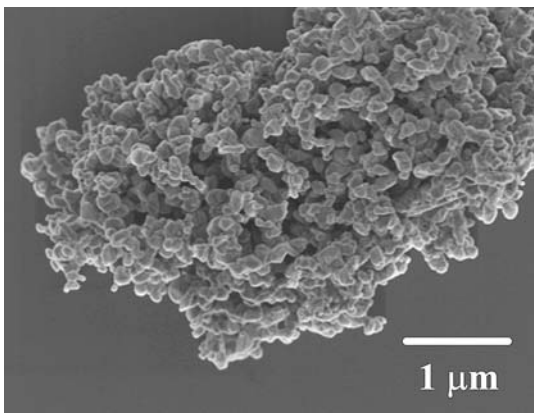

Fig. 1 Representative SEM micrograph of the synthesized powder. Bar = 1 μm

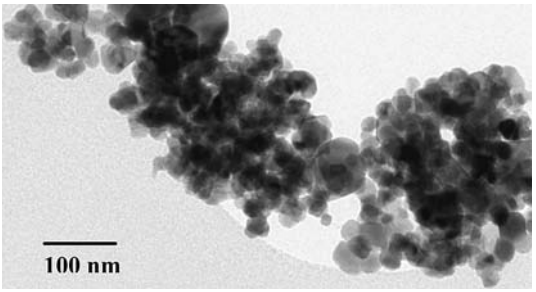

Fig. 2 TEM micrograph of the synthesized powder. Bar = 100 nm

was determined in a previous work [14] that the capacitances are very small and the complex impedance analysis becomes impracticable for samples with this small grain size.

In order to explain possible changes in the doped samples, the potential replacement reactions in the SnO_2 lattice are discussed as follows. With the addition of Co_3O_4 the possible substitution equations, where the Kröger–Vink standard notation is used, are:

$$Co_3O_4 \rightarrow CoO + Co_2O_3 \tag{2}$$

then,

$$CoO \rightarrow Co''_{Sn} + V^{\cdot\cdot}_O + O^x_O \tag{3}$$

$$CoO \rightarrow Co''_{Sn} + 2V^{\cdot}_O + 1/2O_2 \tag{4}$$

$$Co_2O_3 \rightarrow 2Co'_{Sn} + V^{\cdot\cdot}_O + 3O^x_O \tag{5}$$

$$Co_2O_3 \rightarrow 2Co'_{Sn} + 2V^{\cdot}_O + 2O^x_O + 1/2O_2 \tag{6}$$

$$V^{\cdot\cdot}_O + e' \rightarrow V^{\cdot}_O. \tag{7}$$

Cobalt ions bring about an increase in the oxygen vacancies concentration, what enhance the grain growth and prevent the potential barriers from overlapping. In the Nb_2O_5 addition the following equations may apply.

$$Nb_2O_5 \rightarrow 2Nb^{\cdot}_{Sn} + 2e' + 4O^x_O + 1/2O_2 \tag{8}$$

$$V^{\cdot\cdot}_O + e' \rightarrow V^{\cdot}_O. \tag{9}$$

It can be seen that the Nb_2O_5 does not introduce new oxygen vacancies but, since it acts as an electron donor, it contributes to the transformation of $V^{\cdot\cdot}_O$ into $V^{\cdot}_O$. When Fe_2O_3 is present, the following substitution reactions are accounted for:

$$Fe_2O_3 \rightarrow 2Fe'_{Sn} + V^{\cdot\cdot}_O + 3O^x_O \tag{10}$$

$$Fe_2O_3 \rightarrow 2Fe'_{Sn} + 2V^{\cdot}_O + 2O^x_O + 1/2O_2 \tag{11}$$

$$FeO \rightarrow Fe''_{Sn} + V^{\cdot\cdot}_O + O^x_O \tag{12}$$

$$V^{\cdot\cdot}_O + e' \rightarrow V^{\cdot}_O. \tag{13}$$

Then, the oxygen vacancies concentration is increased when Fe_2O_3 is included within the additives. Summarizing, during a thermal treatment, doping agents like Fe and Co ions introduce a great amount of oxygen vacancies in SnO_2, with the associated decrease in the barrier width, hindering the potential barriers from overlap. The concentration of paramagnetic oxygen vacancies was seen to increase in three orders of magnitude, with respect to undoped SnO_2, when cobalt, iron and niobium oxides were added to tin dioxide [7]. It is expected that the doping concentration is very high and then the depletion regions of the grains may not be overlapped.

The response of the sample resistance (R) as a function of time (t) is shown in Fig. 3. Figure 3a shows the electrical response of the non-doped SnO_2 film for temperatures between 150 °C and 450 °C. It can be seen that, after a rapid increase due to oxygen exposure, the electrical resistance evolves with a slower rate. Also, the sensitivity improves with temperature. Note that for non-doped films, after oxygen introduction into the gas chamber, the film resistance increases with temperature. Figure 3b shows the resistance of the doped sample after changing the atmosphere from vacuum (10^{-4} mmHg) into the oxygen one ($t = 0$). The tests were carried out at different temperatures: 275, 350 and 450 °C. In contrast with the behavior of the non-doped samples, doped samples under oxygen atmosphere presented a diminution in the sample resistance with temperature. Moreover at temperatures higher than 350 °C (Fig. 3b), after a fast increase, they showed a diminution in the sample resistance with exposure time (see inset of Fig. 3b). We understand that this is a consequence of the different conduction mechanisms involved in grains with intergrain barriers of Schottky type and grains with overlapped barriers. The diminution of the sensitivity is definitely linked to these results as in the second case the presence of oxygen reflects in a larger conductivity change.

Resistance versus time curves can be understood by considering that intergranular potential barriers are responsible for the observed electrical response. The rapid increase of the resistance, when samples are exposed to oxygen, indicates that equilibrium at the surface is quickly reached. The interaction of oxygen with grain surfaces produces the transfer of electrons from the bulk to the surface. From this process, the barrier height and the depletion width become larger and, as a consequence,

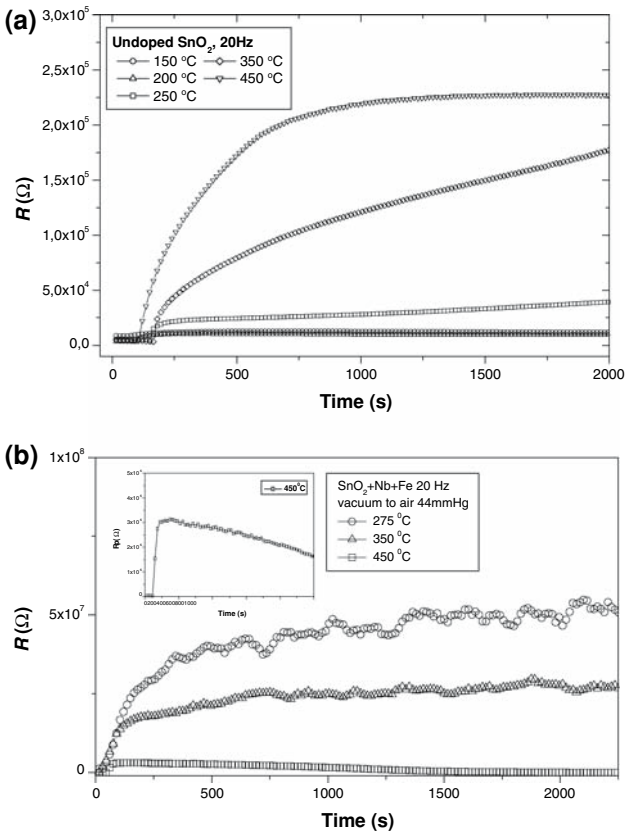

Fig. 3 Electrical response of the sample (R) vs. time (t) when the atmosphere is changed fromvacuum (10^{-4} mmHg) into air (44 mmHg) measured at 20 Hz. In (**a**), the electricalbehavior for undoped samples is shown. The tests were carried out at different temperatures: 150, 200, 250, 350 and 450 °C. In (**b**), the electrical responses for a doped SnO_2 thick film at 275, 350 and 450 °C are shown. In the inset, a detail of the response at 450 °C shows a final slowly resistance decreasing

the sample resistance increases. The subsequent slow change in the electrical response needs a more subtle discussion. In a previous work, we proposed that oxygen diffusion into the grains is responsible for these slow changes in resistance by affecting the oxygen vacancies concentration and the Schottky barrier widths [15, 16].

From Fig. 3a it can be inferred that for non-doped samples, due to the small grain size and the low concentration of donors, the barriers might be initially overlapped. This is consistent with previous observations made at lower temperatures [11]. Interestingly, for doped samples, an improvement in the electrical response was achieved around 300 °C that can be linked to the oxygen diffusion into the grains; the sensitivity increased as shown in Table 1. At temperatures higher than 350 °C the diffusion of oxygen is large enough to provoke the potential barrier overlapping and the decrease in the sensitivity as shown in Table 1. The higher sensitivity for doped samples is registered in the range of 250–300 °C.

Table 1 Sensitivity (S) for different temperatures

	T (°C)	Sensitivity $S = R_{air}/R_{vacuum}$
Doped	175	41
	275	345
	350	126
	400	113
	450	85
Undoped	150	1.5
	200	3
	250	8
	350	54.55
	450	54.43

Figure 4a shows a band model for small grains with a large amount of oxygen vacancies in which barriers of height φ determine the sample conductivity. After the oxygen adsorption on the grain (Fig. 4b), the barriers heights increase relatively fast. Then, due to oxygen diffusion into the grain, the concentration of oxygen vacancies is reduced. As a consequence of both phenomena, the barriers heights and widths became larger and the sample conductivity decreases. At high enough temperatures, due to the diffusion of oxygen into the grain, a diminution of the oxygen vacancies concentration is expected; therefore, the depletion widths might become large enough to overlap (Fig. 4c). After that, as shown in Fig. 4d, the reduction of the oxygen vacancies concentration has the effect of reducing the intergrain barriers heights that the electrons must overcome to flow as the bottom of overlapped potential barriers is raised.

Based on the above discussion, the results of Fig. 3 can be rapidly interpreted. After a first quick increase of the resistance of doped SnO_2 of 50 nm particle size presents a decrease in the resistance when it is exposed to oxygen only at temperatures higher than 350 °C (as already mentioned for undoped thick films this happens at temperatures close to 280 °C). In doped samples, barriers do not overlap easily due to the initial narrow depletion layers; overlapping is only possible when a considerable diffusion of oxygen into the grains takes place (temperatures as high as 350 °C). A great difference with undoped samples is that at lower or moderate temperatures the oxygen diffusion into the grains is not enough as to overlap the potential barriers, and then the resistance increases notoriously.

Table 1 shows the sensitivity $S = R_{air}/R_{vacuum}$ for different temperatures. For the doped film, the maximum value obtained for S is around 300 °C, temperature for which the oxygen diffusion into the grains becomes significant. An increase of sensitivity at this temperature can be a consequence of the reduction in the concentration of oxygen vacancies as the depletion zone of intergranular

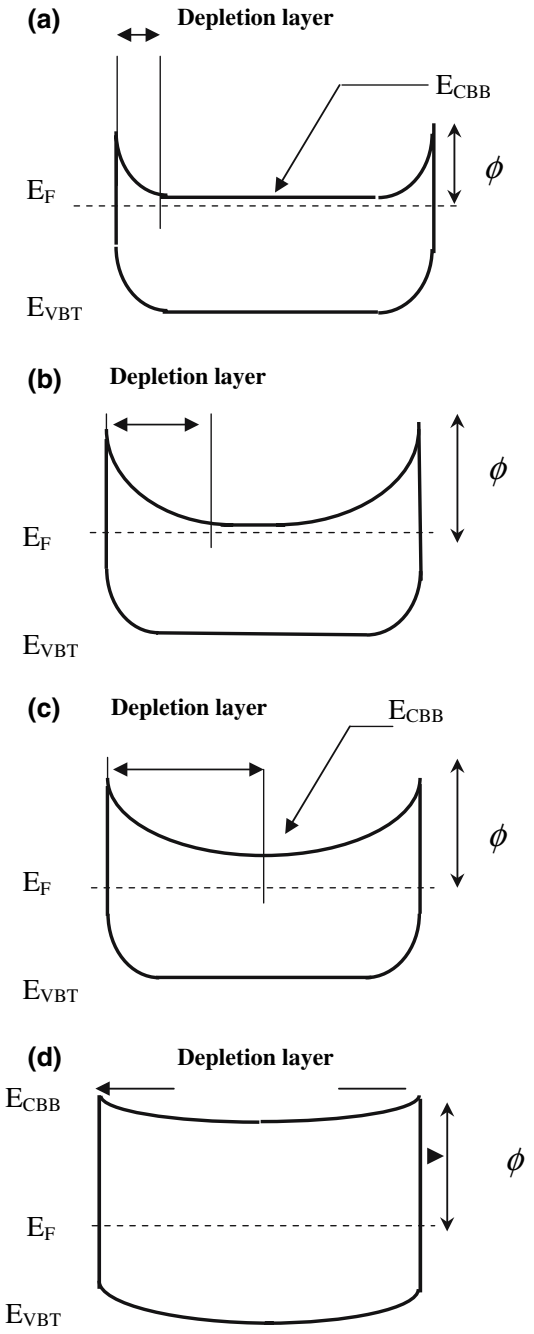

Fig. 4 Band diagrams showing the possible effects of exposure to an oxygen atmosphere. (**a**) Shows the band diagram for a large amount of oxygen vacancies and non-overlapped depletion layers. This represents the behavior of a doped film under vacuum and temperatures lower than ~400 °C. (**b**) Shows the consequences of higher barrier height and lower vacancy concentration. This is the case of a doped film after oxygen exposure that implies higher barriers and a lower amount of oxygen vacancies than in (**a**). (**c**) Band diagram at high enough temperature and depletion widths large enough to produce overlapping. (**d**) Band diagram showing an increase of the bottom of the conduction band due to a strong overlapping

barriers becomes larger and a great increment of R_{air} is observed. Thus, the enhance of the sensitivity for doped SnO_2 films can be attributed to the great amount of oxygen vacancies, to the presence of Fe and Co, and to a decrease in R_{vacuum} linked to the presence of Nb.

The increase in the final resistance with temperature for non-doped films is due to the oxygen adsorption and consequently in the increase in height of already overlapped barriers. On the other hand, for doped films, the decrease in the final resistance under oxygen atmospheres is due to the tunneling current control at low temperatures and by the lowering of the effective barriers due annihilation of oxygen vacancies in depleted grains.

Figure 5a shows the variation of the conductance ($1/R$) as an inverse function of temperature ($1/T$) under initial vacuum conditions for doped samples. The conductance was measured when rising up to 475 °C and decreasing the temperature under vacuum (10^{-4} mmHg). For these temperature ramps, the conductivity was higher during the cooling than during the heating process. This behavior can be associated with the oxygen desorption from the particle surface that produces an increase in the sample conductivity due to a lower potential barrier height.

Next, oxygen was injected into the gas chamber, at 25 °C, until a pressure of 8.4 mmHg was reached (Fig. 5b). The temperature cycles in oxygen atmosphere lead to a decrease of the final conductivity. In all the set of measurements, the conductance after the cycle was lower. This behavior can be associated to the oxygen adsorption in the surface of the particles, which produces a diminution in the conductivity. It was demonstrated that at temperatures lower than 280 °C the oxygen diffusion into the grains is not significant [15, 16]. Note that these results are consistent with the results of Fig. 3b. As can be deduced from Eq. 1, the grains present a narrow depletion layer due to the high value of N_d and then overlapping of potential barriers takes place only at very high temperature despite the small particle size until.

In Fig. 5c, we present the curves of conductance ($1/R$) as a function of $1/T$ under an atmosphere of carbon monoxide for doped samples. The conductance was measured as described above, when rising as well as when decreasing the temperature. In this case the conductivity, in the cooling process, was higher than in the heating process. For temperature ramps below 300 °C, the conductivity was poorer than during the heating process that reached 475 °C. This behavior could be associated with the CO reaction with O_2 adsorbed on the particle surface, which eliminates oxygen and then reduces the barriers height. These results are consistent with those presented in Fig. 5b.

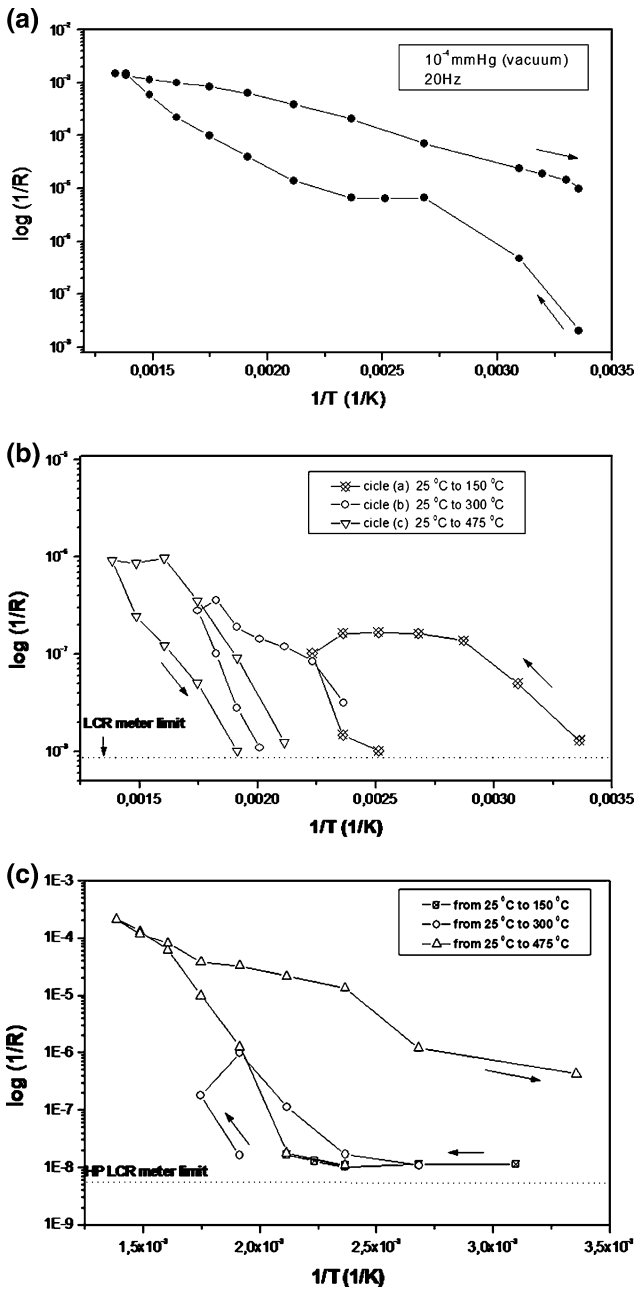

Fig. 5 In (**a**), the conductance (1/R) as an inverse function of temperature (1/*T*) of a doped sample under vacuum conditions is shown. In (**b**), 1/*R* as a function of 1/*T* under 44 mmHg of air is presented; the resistance was measured when raising and decreasing the temperature up to 200, 350 and 475 ºC. Finally, in (**c**), the evolution of 1/*R* as a function of 1/*T* under an atmosphere of 44 mmHg of carbon monoxide are shown

It is well known that for Schottky type potential barriers (assuming non-overlapped barriers) the capacitance is related to the donor density in the bulk, N_d, and the barrier height, φ_B, as [11]

$$C \propto (N_d/\phi_B)^{1/2}. \tag{14}$$

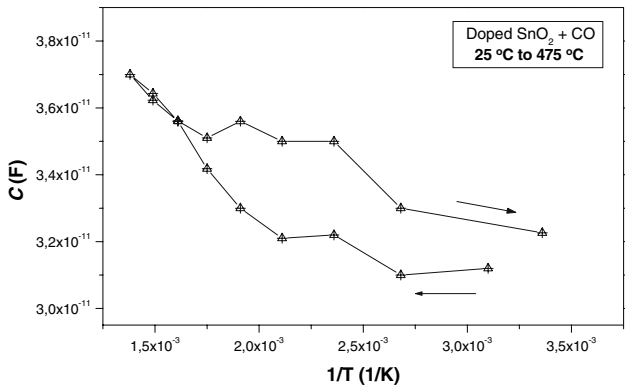

Fig. 6 Capacitance (*C*) vs. 1/*T* curves was measured with the sample under a CO atmosphere. *C* was measured when raising the temperature up to 475 ºC and then cooling down up to room temperature

To gain confidence in the preceding interpretation, in Fig. 6, capacitance (*C*) versus 1/*T* curves when the film was exposed to CO is shown. The capacitance was measured raising the temperature up to 475 °C and then cooling down to room temperature. An increase in *C* during the cooling step is observed. This behavior can be explained if we consider that the resistance is lower during cooling implying a lower φ and a larger N_d. Consequently, the capacitance is greater, as can be determined with Eq. 14.

4 Conclusions

The experimental results reported in this paper lead to the understanding of the influence of Co, Nb, and Fe on the electrical properties of SnO_2 thick film gas sensors. It is possible to conclude the following.

1. Doped films with a mean particle size below 50 nm were calcinated in vacuum and presented non-overlapped potential barriers.
2. Undoped samples show a maximum of the thick films sensitivity (*S*) at temperatures higher than 350 °C. The presence of dopants increases *S* and the maximum value was obtained at temperatures lower than 300 °C.
3. In particular, cobalt and iron ions bring about an increase in the oxygen vacancies concentration. Niobium not only introduces oxygen vacancies but provokes a decrease of the electrical resistance due to its donor character. The enhance of the sensitivity for doped SnO_2 thick films can be attributed to the high concentration of oxygen vacancies, to the presence of Fe and Co, and to the decrease in R_{vacuum} linked to the presence of Nb.

4. The resistance of doped SnO_2 films presents, after a rapid increase, a slow decreasing when the samples are exposed to oxygen at temperatures close to 350 °C indicating that barriers overlapping becomes relevant.

Acknowledgements The authors express their thanks to CONICET and to the National University of Mar del Plata for their financial support and to Héctor Ascencio for his technical assistance.

References

1. R. Parra, J.A. Varela, C.M. Aldao, M.S. Castro, Ceram. Int. **31**, 737 (2005)
2. W. Liu, X. Cao, Y. Zhu, L. Cao, Sens. Actuators B **66**, 219 (2000)
3. N. Yamazoe, Y. Kurokawa, T. Seiyama, Sens. Actuators **4**, 283 (1983)
4. U.-S. Choi, G. Sakai, K. Shimanoe, N. Yamazoe, Sens. Actuators B **98**, 166 (2004)
5. A.C. Antunes, S.R. Antunes, A.J. Zara. A. Pianaro, E. Longo, J.A. Varela, J. Mater. Sci. **37**, 2407 (2002)
6. I.T. Weber, E. Longo, E. Leite, Mater. Lett. **43**, 166 (2000)
7. R. Parra, C.M. Aldao, J.A. Varela, M.S. Castro, J. Electroceram. **14**, 149 (2005)
8. I.T. Weber, R. Andrade, E.R. Leite, E. Longo, Sens. Actuators B **72**, 180 (2001)
9. W. Fliegel, G. Behr, J. Werner, G. Krabbes, Sens. Actuators B **18/19**, 474 (1994)
10. G. Behr, W. Fliegel, Sens. Actuators B **26/27**, 33 (1995)
11. M.A. Ponce, M.S. Castro, C.M. Aldao, Mat. Sci. Eng. B **111**, 14 (2004)
12. M.J. Madou, S.R. Morrison, in *Chemical Sensing with Solid State Devices* (Academic Press, Boston, 1989)
13. X. Wang, S.S. Yee, W.P. Carey, Sens. Actuators B **24/25**, 454 (1995)
14. M.A. Ponce, C.M. Aldao, M.S. Castro, Mat. Sci. Eng. B **123**, 130 (2005)
15. M.A. Ponce, C.M. Aldao, M.S. Castro, J. Eur. Ceram. Soc. **23**, 2105 (2003)
16. G. Blaustein, M.S. Castro, C.M. Aldao, Sens. Actuators B **55**, 33 (1999)